Arch. Metall. Mater. **68** (2023), 4, 1307-1318

DOI: https://doi.org/10.24425/amm.2023.146196

Z. PAN[1], R. LI[1*], Q. ZENG[2]

RESEARCH ON MECHANICAL PROPERTIES OF CARBON NANOTUBES (CNTs) REINFORCED CAST ALUMINUM ALLOY (ZL105)

In order to expand the application range of casting aluminum alloy ZL105, the stirring fusion casting method was used to add carbon nanotubes (CNTs) with different content and aspect ratio into the ZL105 aluminum matrix. And then the effect of the reinforcement on the mechanical properties of the alloy was compared and analyzed. The research results show that the tensile strength and hardness of the carbon nanotube composites with different contents will be improved, but to a certain extent the elongation of the composite material will be reduced, and there is an optimal addition amount. The mechanical properties of composite materials prepared by adding CNTs with relatively small length and diameter are better. There are different forms of reinforcement mechanisms for CNTs to reinforce cast aluminum alloys, and the improvement of composite material performance is the result of the combined effect of multiple strengthening methods. The research has made a meaningful exploration for the realization of carbon nanotube reinforced aluminum matrix composites under the casting method.

Keywords: Cast aluminum alloy; CNTs; Mechanical behavior; Strengthening mechanism; ZL105

1. Introduction

Due to aluminum alloy material has excellent characteristics such as low density and good specific strength, it is widely used in various forming parts obtained by casting and forging. ZL105 aluminum alloy, performance is equal with the 355.0 aluminum alloy of American standard [1], which is widely used in engine cylinder blocks, cylinder heads, bearing supports and other parts in the aerospace and automotive industries because of its good mechanical and heat resistance properties, and good casting and forming capabilities [2]. And carbon nanotubes have the characteristics of high tensile strength and bending strength, low density and thermal expansion coefficient, and good thermal conductivity [3,4], so carbon nanotubes are often used as reinforcements for composite materials.

Carbon nanotubes have been widely used as reinforcements for aluminum matrix composites. CNTs-Al composites with better performance than aluminum matrix materials can be prepared by in-situ synthesis, friction stir and other methods [5, 6]. In addition, Gao et al. used powder metallurgy to prepare carbon nanotube-reinforced 2024Al-based composites, which increased the yield strength of the composites by nearly 1/5 [7]. And the CNTs-Al composite material prepared by Cesar et al. using interlayer technology not only the tensile strength of the material is improved, but also its elastic modulus is greatly improved [8]. Although the carbon nanotubes are added by the above methods can improve the performance of the material, these forming methods have certain limitations, it is not suitable for parts with complex shapes or with internal cavities. And the stirring fusion casting method has the advantages of mature method and convenient operation. It can prepare various parts with complex cavities that meet the requirements of industrial production. This has practical significance for the promotion and application of carbon nanotube-reinforced aluminum alloy composite materials. In addition, studies have shown that the uniform distribution of carbon nanotubes in the aluminum matrix has a great influence on the internal structure of the aluminum matrix, and a good combination between the two will improve the mechanical properties of the composite material [7]. At the same time, due to the poor wettability and dispersibility between the carbon nanotubes and the aluminum matrix alloy, the morphology and content of the carbon nanotubes and the addition process parameters will affect the performance of the composite material during the preparation, it is necessary to

[1] GUIZHOU NORMAL UNIVERSITY, SCHOOL OF MECHANICAL & ELECTRICAL ENGINEERING, CONTRIBUTION CHINA
[2] MANAGER SECTION, GUIYANG HUAHENG MECHANICAL MANUFACTURE CO. LTD CHINA
* Corresponding author: lirong9242001@163.com

change the wettability and dispersibility of the carbon nanotubes in the matrix to increase the bonding area and the bonding force of the composite material interface, so that the performance of the composite material can be improved [9-11].

In this paper, ZL105 aluminum alloy is used as the carrier, and the carbon nanotube-reinforced aluminum matrix composite is prepared by the stirring casting method in the molten state. By adding different aspect ratios and different contents of carbon nanotubes, comparative analysis of their effects on the mechanical properties of carbon nanotube-reinforced ZL105 composites, in order to obtain the best carbon nanotube addition process parameters and discuss the strengthening mechanism of carbon nanotubes on ZL105 aluminum alloy.

2. Experiment

2.1. Material formula

The main element composition of ZL105 alloy complies with the national standard (GB/T 1173-2013), as shown in TABLE 1. Carbon nanotubes (CNTs) are provided by Chengdu Organic Chemistry Co., Ltd., Chinese Academy of Sciences, and their microscopic appearance is shown in Fig. 1. Fig. 1(a) shows that carbon nanotubes are entangled with each other in the form of long fibers and exhibit strong surface energy. Fig. 1(b) shows the TEM of this material, and its structure is a hollow tubular structure.

TABLE 1

ZL105 alloy composition and content (wt%)

Element	Al	Cu	Si	Mg
Content	92.9 (Double zero aluminum)	1.3	5.2	0.6

2.2. Preparation Process

In this experiment, the smelting device was shown in Fig. 2 and the process of smelt was like this. First, in order to obtain the metal melt quickly, the aluminum ingot, copper and silicon blocks and other materials were put into the graphite crucible (except the magnesium ingot). The furnace temperature is set

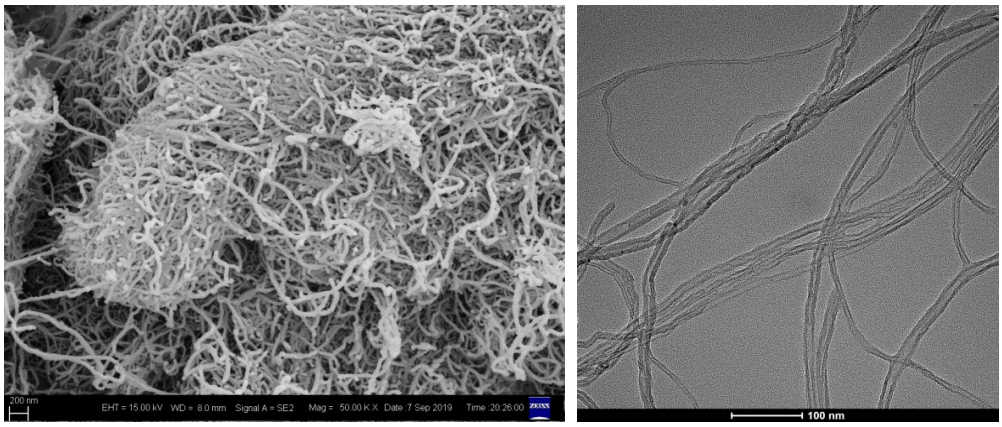

(a) SEM of CNTs (b) TEM of CNTs

Fig. 1. Microscopic morphology of carbon nanotube reinforcement

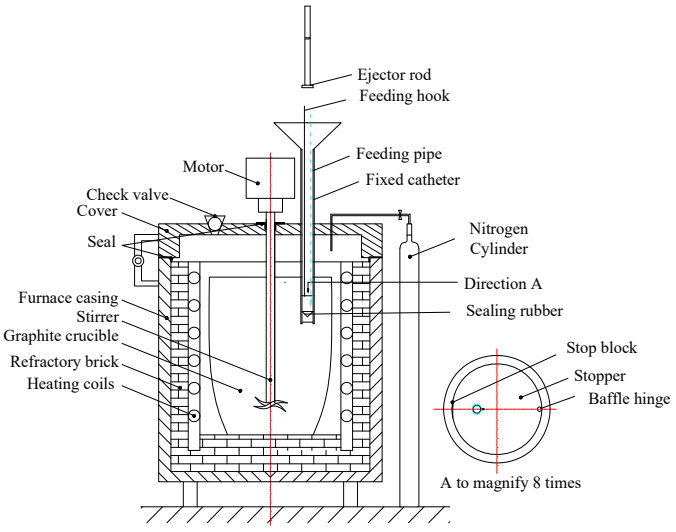

Fig. 2. Schematic diagram of composite material preparation equipment

to 830°C to melt material (About 10% the aluminum ingot was remained). Second, after all the above component materials are melted, the remaining aluminum ingots were added to reduce the temperature to 650-680°C. Then the magnesium ingots are added for melting. Third, when the magnesium ingot was melted, the temperature of the alloy melt was adjusted to 720-750°C. Then stirring motor is started, and nitrogen gas is fed for refining about 20 minutes. Fourth, when the melt was cooled to 550-580°C, the carbon nanotubes wrapped with aluminum foil were pressed into the molten alloy with an ejector rod, and stirred at a speed of 60 rpm with 5 min. Nitrogen need to be fed during the stirring process to isolate the melt from the air. Finally, when the temperature of melt was reheated to 730-760°C, the slag remover is added to clean up the impurities of melt and wait for casting.

The above alloy solution was poured into a metallic die that has been preheated at 200-300°C. The mold structure is shown in Fig. 3(a). After air cooling for one minute, the test bar

(a) Experimental mold (b) Test bar mold

Fig. 3. Experimental mold and sample preparation

mold shown in Fig. 3(b) is obtained. The sample required for the experiment was intercepted and meets the national standard GB/T228.1-2010.

The above-mentioned test bar mold was heat-treated to obtain the final test sample. (Heat treatment process: solid solution temperature 525°C, heat preservation 4 hours; 80°C hot water quenching 2 hours; artificial aging temperature 180°C, heat preservation 4 hours)

2.3. Testing equipment and testing methods

WAW-300 microcomputer servo-controlled hydraulic universal testing machine was used to test the tensile strength of the material, the tensile speed was 2 mm/min, and the loading test force is 10 KN; the electronic extensometer (YYU-5/25) was used to measure the elongation of the material; The HBRV-187.5 electric Brouwer hardness tester was introduced to test the hardness of the material, the test force was 612.9 N, and the pressure holding time is 32S; 3 sets of MPD-2 metallographic grinding and polishing machines with different sandpaper particle sizes were used, and the samples were polished one by one on sandpaper with coarse to fine grain size. Then the diamond paste was used for sample polishing, and the prepared aluminum alloy etch solution (ϕ < HF:HCl:HNO_3:H_2O >= 1:1.5:2.5:95) was used to etching the sample for 5 minutes, 4XC-MS metallographic microscope is used to observe the surface metallographic morphology of the corroded sample; JEM-2100F scanning electron microscope was used to observe the fracture morphology of materials and use EDS to test the distribution of each element; The JSM-7001F transmission electron microscope was used to measure the internal structure of the composite material and the content of each element component was obtained through the spectrum inspection.

2.4. Experimental program

In order to determine the best process for carbon nanotubes to enhance the mechanical properties of ZL105 aluminum alloy, and to obtain the optimal combination of carbon nanotube addition amount and type, carbon nanotubes with different contents and different aspect ratios (CNTs1: tube diameter 5-15 nm, length 10-30 um; pipe diameter 30-80 nm, length <10 um) were added to the alloy system. Samples of carbon nanotubes with different aspect ratios and contents were numbered. No. 0 means no carbon nanotubes, No. 1-5 means carbon nanotube materials with a large aspect ratio, and No. 6-10 means carbon nanotube materials with a small aspect ratio. The specific scheme was shown in TABLE 2.

TABLE 2

List of experimental sample numbers and component contents.

Sample number	Types of CNTs	wt.%
0	Not added	0.00
1	CNTs1	0.50
2	CNTs1	0.75
3	CNTs1	1.00
4	CNTs1	1.25
5	CNTs1	1.50
6	CNTs2	0.50
7	CNTs2	0.75
8	CNTs2	1.00
9	CNTs2	1.25
10	CNTs2	1.50

3. Experimental result

3.1. Mechanical properties

Fig. 4 is the curve of the tensile strength of the composite material. It can be seen from the figure that the strength of the CNTs-Al composite material after the addition of carbon nanotubes had been greatly improved compared to the matrix ZL105 aluminum alloy without carbon nanotubes. With the increasing the content of carbon nanotubes added, the tensile strength of the two groups of materials both increased first and then decreased. And when the addition amount was 1.25%, the maximum value was obtained (CNTs1: 312.41 MPa; CNTs2: 326.33 MPa, the strength difference between the two was 13.92 MPa), compared with the base material, the tensile strength increases by 5.81% and 10.53%. Comparison with both groups of samples, it was found that the strength curve of the material with CNTs1 was smoother than the material adding

CNTs2. And the maximum difference of strength was shown at the 0.75% of content for different CNTs, which maximum value was 15.24 MPa. In the whole set of experiments, only when the addition amount is 0.5%, the strength of the material with CNTs2 added was lower than the strength of the material with CNTs1 added. When the addition amount was 1.25% on the nearest two sides, the tensile strength of the material added with CNTs2 changes more drastically than the material added with CNTs1, and it also showed that CNTs2 can better enhance the strength of the composite material than CNTs1.

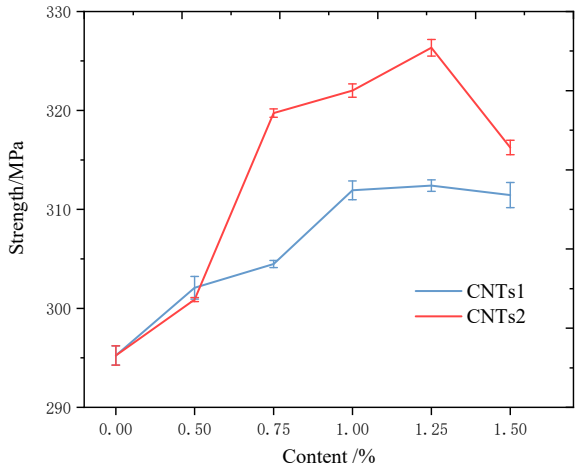

Fig. 4. Effect of different content and types of carbon nanotubes on the tensile strength

Fig. 5 was the elongation change curve of the composite material. It can be seen from the figure that the addition of CNTs can cause the reduction of the elongation of the composite material, only when CNTs2 with a mass fraction of 1.5% was added, the elongation of the composite material was greater than that of the matrix material. As the amount of CNTs increases, the elongation curve approximates to a "U" shape. When the addition amount was 1%, the elongation of the composite with CNTs1 reached the lowest value of 2.69%, and the elongation relative to the matrix material was reduced by 14.06%. When the addition amount was 0.5%, the elongation of the composite material with CNTs2 was at a minimum of 2.88%, and the elongation relative to the matrix material was reduced by 7.98%. In addition, the elongation difference of this material was only 0.03% when the addition amount was 0.5% and 1%. For two different reinforcements, the elongation of the two materials would increase when the additive content exceeds 1%. In the whole set of experiments, the elongation of the composite with CNTs2 was always greater than the elongation of the composite with CNTs1.

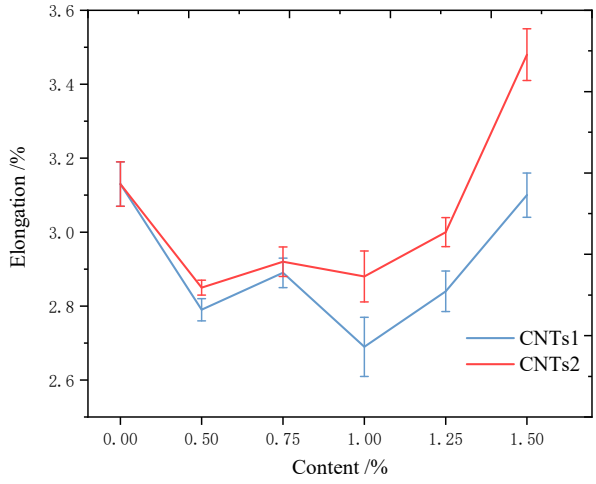

Fig. 5. Effect of different content and types of carbon nanotubes on material elongation

Fig. 6 is the hardness change curve of the composite material. It can be seen from the figure that the hardness increase value of CNTs to the ZL105 aluminum alloy material was kept within 10HB. With the change of the amount of addition, the shape of the hardness curve was almost opposite to the elongation curve, that was, the material with low hardness had a large elongation, which was consistent with the properties of the actual material. The hardness of the composite material with CNTs1 added at 1% achieved the maximum value (77.26 HB), while the composite material with CNTs2 added at 1.25% hardness achieved the maximum value (75.99 HB), compared with the base ZL105 aluminum alloy material, the hardness of the two materials increased by 12.79% and 10.93%, respectively. When the addition amount of reinforcement was only 1.25%, the composite material with CNTs2 added was harder than CNTs1. With the increasing the amount of addition, the hardness values of the two materials have little difference, but when the addition amount was 1%, the maximum difference between the two was 2.64 HB.

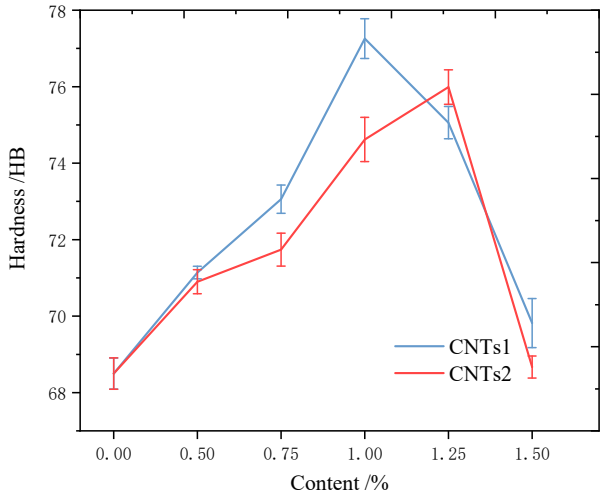

Fig. 6. Effect of different content and types of carbon nanotubes on the hardness

Judging from the three performance results of the above-mentioned composite materials with different aspect ratios, the change trend of the mechanical properties of the two was basically the same, the elongation and hardness were not significantly different, and there was a significant difference in strength. Adding CNTs can improve the strength and hardness of the base material ZL105, but the elongation of the material would be reduced. The strength and elongation of CNTs2 composites were better than those of CNTs1 composites, but the hardness

performance of CNTs2 was not as good as that of CNTs1, and the effect of the two on the matrix material is similar. On the whole, CNTs2 had a better effect than CNTs1 in improving the mechanical properties of ZL105 aluminum alloy.

3.2. Microstructure

3.2.1. Metallographic structure

Fig. 7 are the metallographic diagrams of the ZL105 aluminum alloy composite reinforced with carbon nanotubes with different content and aspect ratio. It was obvious that adding different content and different types of carbon nanotubes had a great influence on the metallographic structure of the material. Fig. 7(a) showed the metallographic structure of the material without carbon nanotubes. The dendrites were slightly coarse, with a small amount of small black spots and small black flaky strengthening phase precipitates, which precipitated along part of the grain boundaries and were randomly distributed in the metallographic structure. Fig. 7(b) showed that the crystal grains in the metallographic structure at this content scatter and spread along the central gathering point, and the individual crystal grains were closely connected together. However, as the crystal grains grow, the grain boundary slightly away from the central point was not obvious, and the interface energy was weakened, the connection between the crystal grains was not tight. In the Fig. 7(c), most of the strengthening phases were uniformly precipitated along the grain boundaries, and the structure distribution was relatively uniform, but there was a situation where some strengthening phases were not precipitated and the grain boundaries were missing. At the same time, obvious segregation occurred, and a

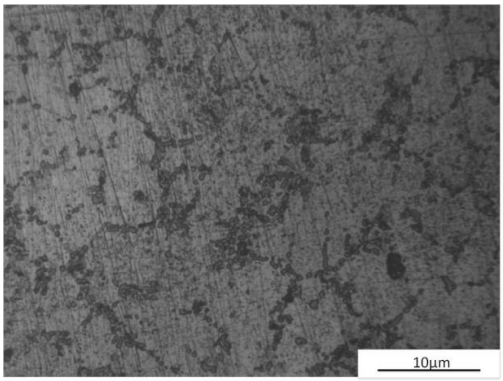

(a) Sample 0

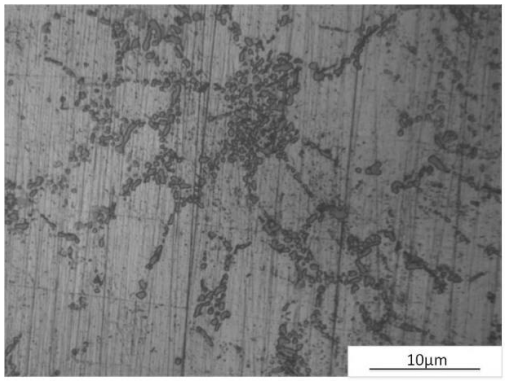

(b) Sample 4

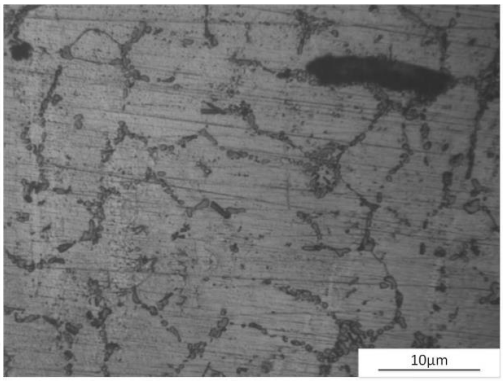

(c) Sample 5

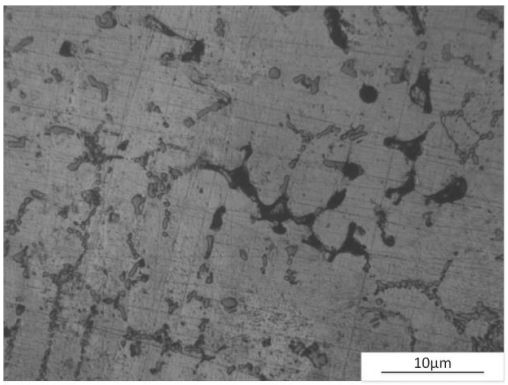

(d) Sample 9

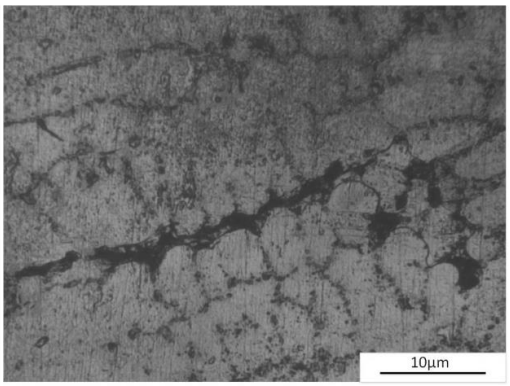

(e) Sample 10

Fig. 7. Metallographic diagrams of ZL105 aluminum alloy composite with different aspect ratios and contents of carbon nanotubes

piece of black long strip of material was gathered on the grain boundary. In the Fig. 7(d), only the middle part of the strengthening phase precipitates more, the overall precipitation was not sufficient and uneven, and the intermittent grain boundaries formed, only a few parts were well connected, but the overall connection between the grains was not complete. At this time, the segregation phenomenon had a tendency to aggravate, until the content was added to 1.5%, a large number of strengthening phases precipitate and aggregate along the grain boundaries, forming an obvious thick and long black strip. As a result, the crystal grains were aggregated and coarse, resulting in uneven and not tight interface contact, as shown in the Fig. 7(e).

Comparing the metallographic diagrams of adding two carbon nanotubes with different aspect ratios, it was found that the composite material with CNTs2 was more prone to segregation. It because the aspect ratio of CNTs1 was larger than that of CNTs2, and carbon nanotubes with a larger aspect ratio were more likely to entangle together during the process of adding. Since CNTs2 had a small aspect ratio, and a small bond between the two carbon nanotubes, it can be relatively easily dispersed to the grain boundary to precipitate. At the same time, relying on its own strong interfacial energy characteristics, more strengthening phases were attracted to gather here.

3.2.2. Fracture morphology

It is obvious from Fig. 8 that the fracture morphology of the material obtained by adding different aspect ratios and different contents of carbon nanotubes was quite different. Fig. 8(a) was the SEM image of the fracture of the ZL105 aluminum alloy as the base material of this experiment. From a macro point

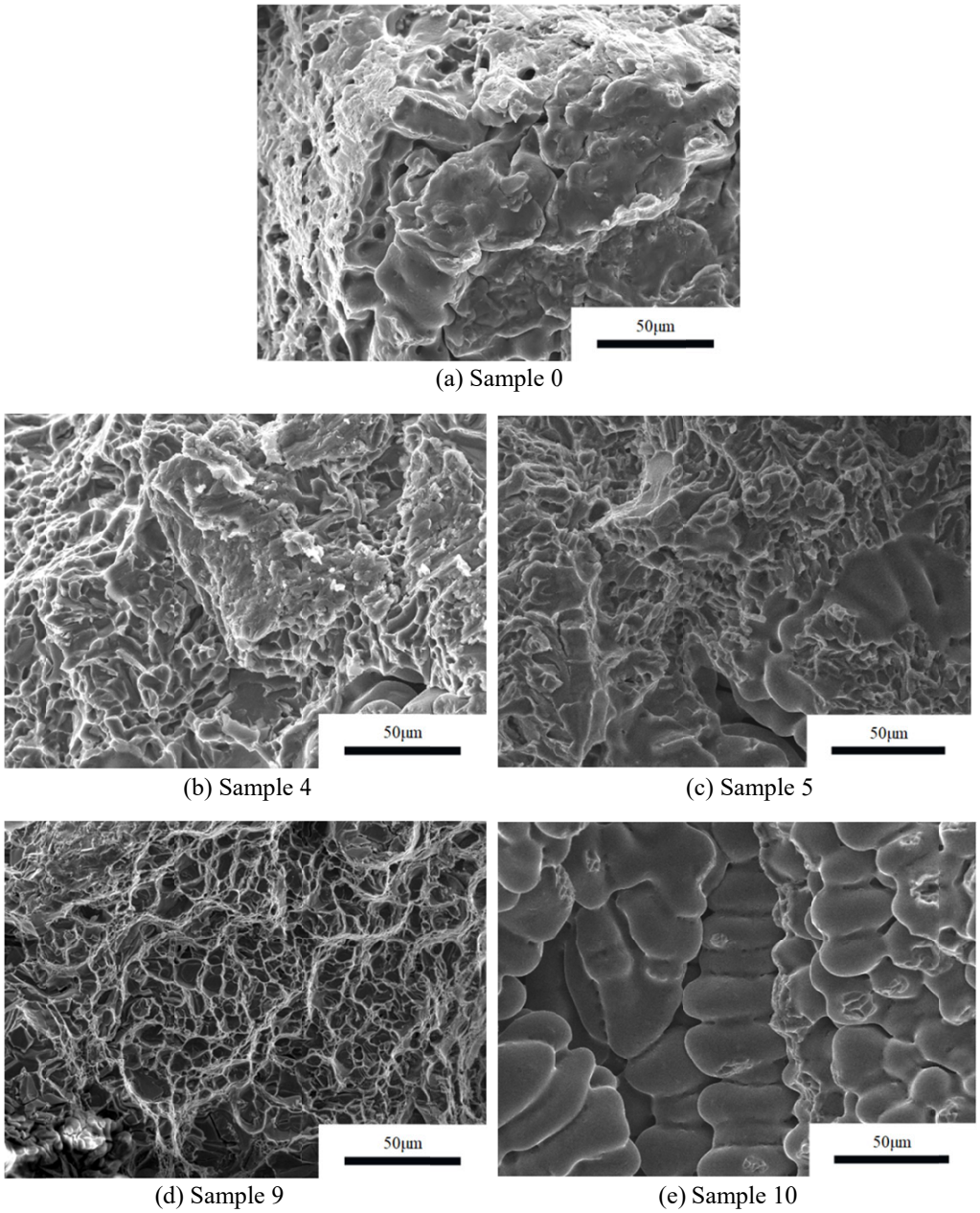

(a) Sample 0

(b) Sample 4

(c) Sample 5

(d) Sample 9

(e) Sample 10

Fig. 8. SEM image of the fracture surface of ZL105 aluminum alloy reinforced with different aspect ratios and content of carbon nanotubes

of view, the fracture morphology showed a middle high and two low sides, and many circular black holes were distributed on the surface, the fracture morphology was relatively round and almost no ravine was formed, and the actual macroscopic fracture of the sample was inclined at 45°, which was a typical ductile fracture feature. When CNTs1 with a content of 1.25% was added, small dimples gradually appear in the fracture, with smooth deep gaps and elongated and thinned tearing edges locally, and the overall appearance was uneven. And white flakes were attached to the protrusions as shown in Fig. 8(b). The actual fracture of the sample was a flat surface, with part of the tearing edge raised on it, and there were flakes on the tearing edge that are consistent with the microscopic fracture morphology, which was the performance of brittle fracture. Fig. 8(c) is a fracture diagram of a CNTs1 composite with a 1.25% content. The figure showed a long tearing edge on the left side, there was a deep and long black elongated hole below it, and the vicinity was smooth and edgeless, where a local ductile fracture is shown. Fig. 8(d) showed the fracture morphology of the CNTs2 composite with a content of 1.25%. There were many bright tearing edges in the morphology, a large number of small dimples are evenly distributed on the surface of the fracture. A crack phenomenon in the bottom of the local socket, and the brittle fracture characteristic of the fracture was the most obviously, and it was consistent with the above-mentioned mechanical properties, high strength, high hardness and low elongation. The fracture morphology of Fig. 8(e) showed the characteristics of a deep groove with low middle and high sides, and all of them are closely connected by numerous short rod-shaped and spherical structures. The surface of individual short rod-shaped structure was a little damaged. This sample has the best toughness and higher elongation, but the result was low strength and low hardness.

From the above-mentioned microstructure morphology, adding different contents and types of CNTs will affect the structure morphology of the composite material. The fracture morphology of the composites with CNTs1 added did not change significantly with the increase in the amount of addition, while the fracture morphology of the composites with CNTs2 was greatly affected by the addition, and the structure of the composite morphology changes from a dimple shape to a short ball stick shape.

4. Discussion

The foregoing experimental results showed that after the adding the carbon nanotubes, the mechanical properties of the composite material was improved. In order to explore the enhancement mechanism of carbon nanotubes to ZL105 material, this section starts from the experimental results and constructs a related theoretical model to discuss the enhancement mechanism. From the research results, the strengthening mechanisms of carbon nanotube-reinforced aluminum matrix composites mainly included deformation strengthening, dispersion strengthening, dislocation strengthening and solid solution strengthening, and these strengthening mechanisms were analyzed.

4.1. Deformation strengthening

When the material is stretched by an external force, it will produce tensile deformation. At this time, the internal structure of the material plays a major role in strengthening. The fracture diagram of sample 9 was partially enlarged, and it was found that the fracture form was different from the typical brittle fracture. The bottom of the fracture surface had a flat boss, which was flat but there were certain cracks, and the side surface was smooth and flat. The whole dimple presents a “half eggshell” structure, as shown in Fig. 9(a). Fig. 9(b) was a model diagram of one of the dimples, and its cross-sectional view can clearly show that the special large platform fracture morphology was produced after the dimple fracture. This phenomenon occursed because the addition of carbon nanotubes would form numerous microscopic interfaces with preferential nucleation positions in the melt. At the same time, the carbon nanotubes themselves also had good thermal conductivity, and the degree of subcooling in the area where the carbon nanotubes exist also would increase. Therefore, micro-cracks would be formed preferentially in this area, and external energy would be transferred and concentrated here, so that the micro-cracks would continue to grow to a certain extent and then fracture [12].

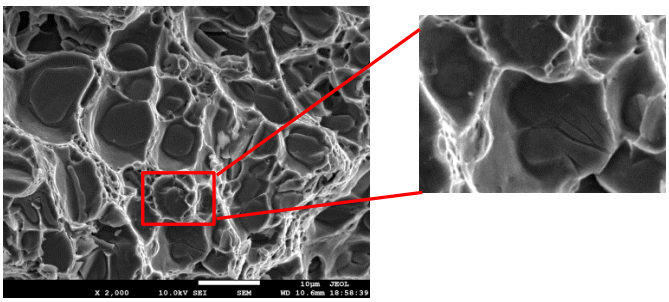

(a) Partial enlarged view of the fracture of sample 9

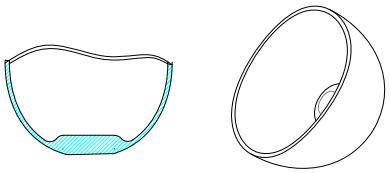

(b) Sample 9 "Eggshell"-shaped dimple model diagram

Fig. 9. Fracture surface of sample 9 and model of the “Eggshell”

The growth and fracture mechanism of the “egg shell” of the sample in this experiment can be explained by the model in Fig. 10, which is taking one of the micro crack as an example. When the composite material is subjected to external force, micro crack appear in the local area where the carbon nanotubes exist. After further stretching, the micro crack will gradually aggregate and grow into visible micro-holes. When it continues to load to the maximum strength of the composite material, it will break along the middle of the micro-hole, forming a tearing edge at the crack of the micro-hole, and this micro-hole can be regarded as an “egg shell”. Song et al. [13] used the finite element method to establish the

stress model of the eggshell. The study found that the characteristic of the eggshell loading that the side of the eggshell is more stressed than the bottom. Therefore, the position where the egg shell breaks is on the side part, which is the same as the breaking mechanism in the above-mentioned "egg shell" model. Fig. 9 showed that the bottom of the micro-hole was relatively flat and hardly affected by the load. However, it was found that there were cracks at the bottom edge of some micro-holes, and there was a tendency to extend at the bottom. It is because when the material was loaded, the growing micro-holes will transfer the load along the side of the hole to the bottom of the hole. At this time, the internal load transfer of the composite material was the combined action of the side and bottom of the micro-hole formed by tensile fracture.

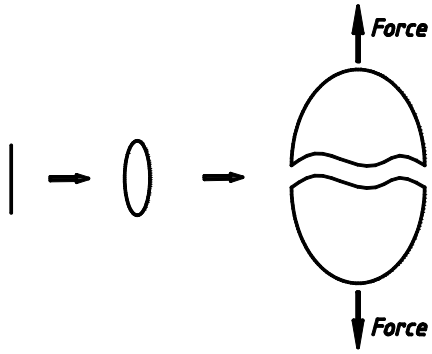

Fig. 10. Sample 9 "Eggshell"-shaped dimple growth and fracture model

In order to further explain the characteristics of this fracture, a microscopic fracture diagram was used to explain it, as shown in Fig. 11. Fig. 11(a) was a cross-sectional view of the brittle fracture. The fracture was uneven and jagged, with stress-concentrated tips, where micro cracks generate nucleation sites [14]. Fig. 11(b) is a schematic diagram of the fracture section of sample 9. The fracture structure and bottom fracture form were both shown brittle fractures, so the strength and hardness of the composite material can be guaranteed. In addition, the convex platform and the concave structure, which was parallel to the fracture level of material, can effectively overcome the problems of stress concentration during the stretching process. It can mitigate the degree of reduction in the elongation of the material. Therefore, this composite material was different from traditional brittle materials. It does not sacrifice excessive elongation in exchange for increased strength and hardness. It was a brittle material with a small amount of toughness.

4.2. Dispersion strengthening and load transfer

Fig. 12 is a scanning electron microscope image of 9 slices of the sample. The surface of the sample after the thinning treatment had curved and damaged structures with different shapes, and the damaged positions were evenly distributed, as shown in Fig. 12(a). Fig. 12(b) was an EDS at this location, showing that the C element was more uniformly dispersed in the matrix Al, and the C element was distributed in the damaged position. The study found that the uniform dispersion of carbon nanotubes was the key to enhancing the performance of composite materials [15]. Therefore, the C element was the main element that caused the structure and performance of the composite to be enhanced. The part C in Fig. 12(a) was partially enlarged, and it is found that the structure presents a "C" shape. This kind of hook-shaped structure will increase the stability of the internal bonding of the material, and play a role in transmitting the load inside the material, thereby improving its mechanical performance. Fig. 12(d) is the C-Al EDS, it was found that this structure was mainly composed of C element, so C element may promote the generation of irregular structure to increase the internal load transfer capacity of the composite material. Fig. 12(e) is the enlarged view of D zone in Fig. 12(c). It was shown that the C elements were closely arranged in spherical fine particles to form a sheet-like structure, which had a filling and strengthening effect on the composite material [9].

4.3. Interface strengthening and dislocation strengthening

Fig. 13 is a transmission electron microscope image of sample 9. The point E in Fig. 13(a) was a block structure, embedded in the matrix, and the interface with other tissues was flat, and the interface bonding condition was good. The spectrum

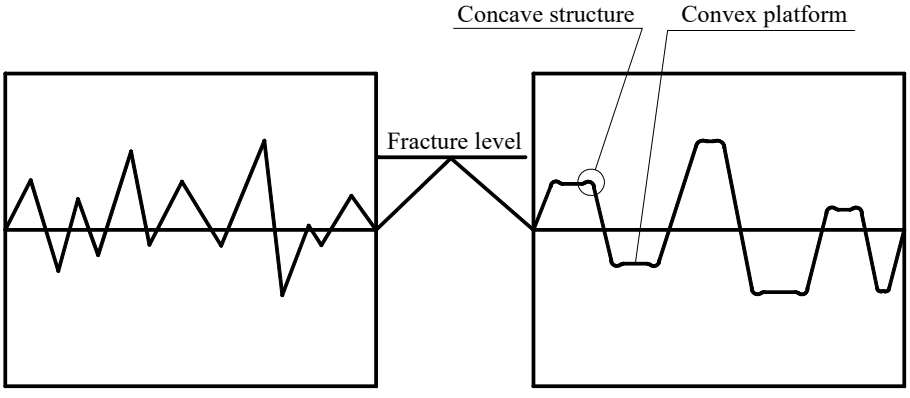

(a) Schematic diagram of brittle fracture (b) Schematic diagram of sample 9 fracture

Fig. 11. Microscopic fracture mode (section view)

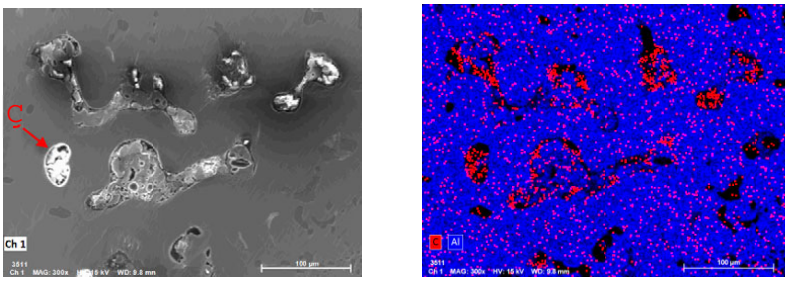

(a) Sample 9 slice thinning SEM (b) Figure (a) C-Al EDS

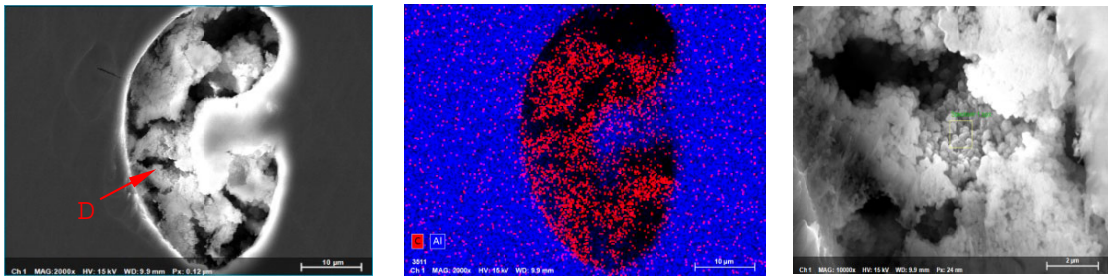

(c) Enlarged view at C zone (d) Figure (c) C-Al EDS (e) Enlarged view at D zone

Fig. 12. SEM image and EDS image of sample 9 slice thinning

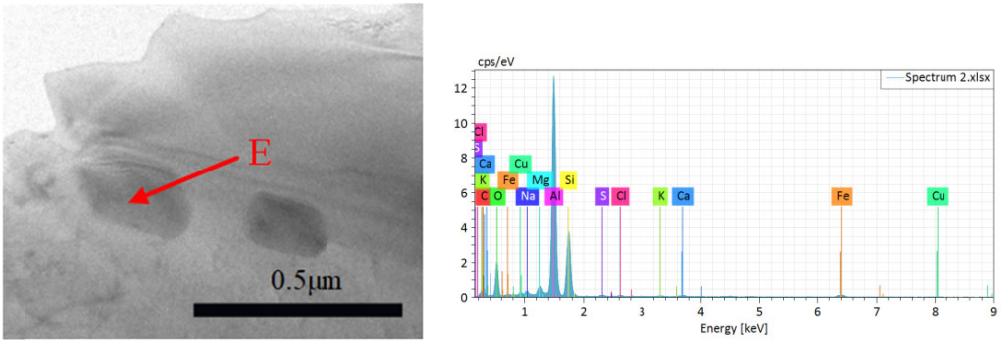

(a) Sample 9 TEM (b) E zone spectrum

Fig. 13. TEM and E zone spectrum of sample 9

of this structure is shown in Fig. 13(b). This region was mainly composed of Al-Si and C-O phases, and the content of its main key elements was shown in TABLE 3. From the content of each element in TABLE 1, it is known that the content of Al and Si elements in ZL105 aluminum alloy was the largest. At the same time, the Al-Si phase also constitutes the basic phase of ZL105 aluminum alloy, providing a basic Al-Si interface for composite materials. TABLE 3 shows that there are more C and O elements. The existence of O element was because the oxygen in the air was sucked into the alloy solution when the base alloy material was melted at high temperature. When carbon nanotubes were added later, O_2 in the matrix material was decomposed by the carbon nanotubes and absorbed into the composite material [16], and formed the C-O phase. Studies had shown that the molecular bonds between CO_2 were easily broken at high temperatures, which leaded to the decomposition of CO_2 and a gasification reaction. This reaction will generate adsorptive ketone C·O and ketene C·CO on the carbon surface. The specific structure forms >C=O and >C=C=O, forming stable carbon bonds [17]. Adsorbent groups played a key role in the connection of the internal interface of the composite material, so that the mechanical properties of the composite material were improved.

TABLE 3

Contents of main elements at point E

Element	Wt.%	At.%
Al	33.70	23.60
Cu	1.10	0.30
Si	14.30	9.60
Mg	1.10	0.80
C	26.00	40.90
O	18.90	22.30

Fig. 14(a) is a TEM photograph of sample 9. The figure shows that there were many randomly scattered irregular flakes and long strips, which increase the connections between the materials. Fig. 14(b) is an enlarged view of F zone in Fig. 14(a). It was found that there were three overlapping parts of the tissue

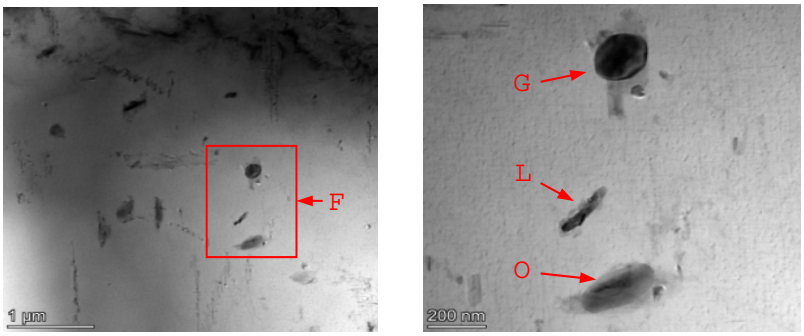

(a) Sample 9 TEM (b) Enlarged view at F zone

Fig. 14. Sample 9 and its enlarged view

in the figure. The solid disc-shaped and hollow-tube tissues at G zone overlap, the tubular and long solid tissues at L zone were combined, and the hollow tube and elliptical sheet-shaped tissues at O zone overlap. These tissues were combined together in an embedded manner, and the tissues at G and O zones overlap more and have a larger bonding area, so they can provide connection and transfer for the improvement of the mechanical properties of the material. These stacked parts increase the dislocation density of the composite material, reduce the number of mobile dislocations, and thus the strength of the composite material was improved [18]. In addition, it was found that the tubular tissues at G and L zones present an angular distribution of about 120°. This intricately distributed form can effectively hinder the slippage of the internal tissue of the material along the interface, and can effectively transfer the load to improve the mechanical properties of the material.

4.4. Solution strengthening

When the supersaturated solid solution exceeds the self-dissolving ability of the material matrix during the chilling process, solute will get rid of solid solution and precipitate to the grain boundary. It increases the difficulty of grain boundary slip, and then realizing the solid solution strengthening of the material. Because the carbon nanotubes were resistant to high temperatures and had good thermal stability, they will not be slightly melted with other metals during heat treatment. At this time, CNTs would get rid of solid solution and precipitated as solute. Fig. 15 is the metallographic morphology of sample 9. From Fig. 15(a), it can be seen that there was a phenomenon of tissue shedding at M zone, while at N zone, there was a strengthening of the structure to segregate to the grain boundary, and the irregular long precipitates were concentrated in the grain boundary. It played a role in connecting the grains. At the same time, this solution strengthening form in this experiment had complementary significance to the other strengthening forms mentioned above [19]. Fig. 15(b) shows that the location of the tissue exfoliation was short and straight and there was crystal grain aggregation, This phenomenon was due to the fact that when an external force was applied, all energy would be induced to gather here. When the energy it can absorb was exceeded, the precipitated phase would fall off along the grain boundary, which would cause the complete structure of the material to be destroyed and fail. However, the precipitation strengthening area of this sample reinforcement was larger than the shedding failure area, so the overall enhancement effect was shown. And at this time, the distribution and the degree of aggregation were also moderate, which can play a relatively maximum enhancement effect.

The above process can be further explained by the reinforcement-stripping model shown in Fig. 16. Because the heat treatment process could generate precipitation powder [20], the

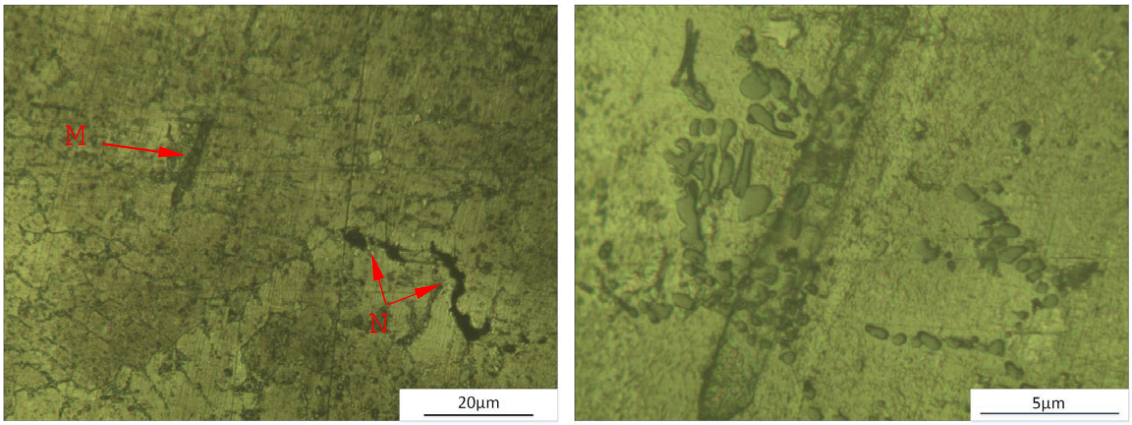

(a) Metallographic diagram (b) Metallographic magnified at M zone

Fig. 15. Metallographic morphology and its enlarged view

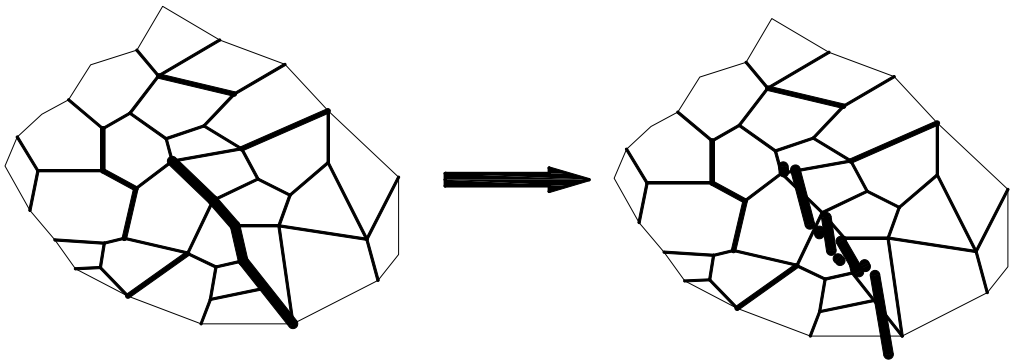

Fig. 16. Reinforcement-peeling model

strengthening phase was precipitated along the grain boundary, but there was a partial segregation phenomenon. Carbon nanotubes also could exist on the grain boundaries. With their own high-energy characteristics, more precipitates were induced to accumulate at the grain boundaries. At this time, there was a limit to the degree of aggregation. When the aggregation reached this limit, the precipitated phase would become thicker, causing the degree of bonding with the matrix to decrease and fall off. In addition, the location of precipitation and aggregation depended on the degree of dispersion of carbon nanotubes, and the timing of exfoliation depended on the degree of aggregation and the size of the external force on the material. The precipitate can be used as a strengthening phase to strengthen the material in a small amount, but it would have the opposite effect if it exceeded a certain amount. This also explains the reason for the decrease in the strength of the composite material with 1.5% carbon nanotubes added relative to 1.25% carbon nanotubes.

In summary, the structure, elements and interfaces in the internal structure of the composite material all play a role in enhancing the performance of the composite material to a certain extent. The coupling and synergy between the strengthening methods such as structural deformation strengthening and uniform dispersion strengthening produced by them made the mechanical performance to the greatest extent possible.

5. Conclusions

The strengthening effect of adding carbon nanotubes with different aspect ratios and contents to the matrix ZL105 aluminum alloy was researched. Through the comparison of multiple sets of experiments, the best carbon nanotube addition combination was obtained, and the strengthen mechanism was proposed. The following conclusions were obtained through research.

1. The addition of carbon nanotubes will change the mechanical properties of cast aluminum alloy ZL105, and the addition of carbon nanotubes had a significant impact on the properties of composite materials. When the added mass fraction was 1.25%, the maximum tensile strength and hardness would be achieved, but the elongation would be reduced; the types of carbon nanotubes added had little effect on the performance of the composite material.

2. The microstructure of cast aluminum alloy ZL105 was affected by the content of carbon nanotubes and the aspect ratio. When the content was 1.25%, the structure was the most delicate and the strengthening effect was the best, and carbon nanotubes with smaller aspect ratio can better improve the microstructure of the material.

3. Carbon nanotube-reinforced ZL105 aluminum alloy composites mainly had four types of strengthening methods: deformation strengthening, dispersion strengthening, dislocation strengthening and solution strengthening. The comprehensive coupling effect of these strengthening methods had achieved the improvement of the mechanical properties of the composite material.

Acknowledgments

This research was financially supported by the Guizhou Industry Simulation Design & Innovation Center (QKZYD NO.[2016]4006). Moreover, this research was also financially supported by Doctoral Research Foundation of Guizhou Normal University (2017). This research was also supported by Guizhou Education Department Science and Technology Research Project Serve for the"Four new"and "Four modernization" (QJJ [2022] No. 005).

REFERENCES

[1] R.J. Peng, Modern Comprehensive Mechanical Design Manual, Beijing Press (1999).

[2] Z.P. Wang, S.G. Wang, The effect of artificial aging temperature of ZL105 aluminum alloy on mechanical properties, Mechanic (thermal processing) (02), 26-27 (1995).

[3] R.H. Ding, Research status of carbon nanotube reinforced metal matrix composites, Thermal Processing Technology **46** (14), 11-14 (2017).
DOI: https://doi.org/10.14158/j.cnki.1001-3814.2017.14.003

[4] S. Zhao, Z. Liu, X.B. Zhang, Research on the technology and properties of carbon nanotubes reinforced aluminum matrix composites, Casting Technology (02), 135-138 (2006).

[5] X. Zhao, L.M. Ke, W.P. Xu, G.P. Liu, Research on the microstructure and properties of aluminum matrix composites prepared by

friction stir processing, Thermal Processing Technology **39** (20), 76-79 (2010).

[6] H.P. Li, PhD thesis, In-situ synthesis of carbon nanotubes on aluminum matrix and the microstructure and properties of composite materials, Tianjin University, Tianjin, China (2008).

[7] Y.F. Gao, L.J. Guo, W.G. Wang, G.F. Zhang, Microstructure and properties of carbon nanotubes reinforced 2024 Al-based composites, Thermal Processing Technology **44** (22), 1-5 (2015). DOI: https://doi.org/10.14158/j.cnki.1001-3814.2015.22.001

[8] C.A. Isaza, M. Ledezma Sillas, J.E. Meza, J.M. Herrera, J.M. Ramírez, Mechanical properties and interfacial phenomena in aluminum reinforced with carbon nanotubes manufactured by the sandwich technique, Journal of Composite Materials **51** (11), 1619-1629 (2016).
DOI: https://doi.org/10.1177/0021998316658784

[9] B. Chen, J. Shen, X. Ye, L. Jia, S. Li, J. Umeda, M. Takahashi, K. Kondoh, Length effect of carbon nanotubes on the strengthening mechanisms in metal matrix composites, Acta Materialia **140**, 317-325 (2017).
DOI: https://doi.org/10.1016/j.actamat.2017.08.048

[10] M. Majid, G.H. Majzoobi, G.A. Noozad, A. Reihani, S.Z. Mortazavi, M.S. Gorji, Fabrication and mechanical properties of MWCNTs-reinforced aluminum composites by hot extrusion, Rare Metals **31** (4), 372-378 (2012).
DOI: https://doi.org/10.1007/s12598-012-0523-6

[11] X.X. Zhang, H.M. Wei, A.B. Li, Y.D. Fu, L.Geng, Effect of hot extrusion and heat treatment on CNTs–Al interfacial bond strength in hybrid aluminium composites, Composite Interfaces **20** (4), 231-239 (2013).
DOI: https://doi.org/10.1080/15685543.2013.793093

[12] Q. Xu, X.S. Zeng, G.H. Zhou, Mechanical properties of CNTs/AZ31 magnesium-based composites prepared by the bell jar immersion block casting method, Chinese Journal of Nonferrous Metals **20** (02), 189-194 (2010).
DOI: https://doi.org/10.19476/j.ysxb.1004.0609.2010.02.004

[13] H.Z. Song, J. Wang, J.A. Ye, A finite element study on the loading characteristics of egg shells, Journal of Zhejiang University (Agriculture and Life Sciences Edition) (03), 350-354 (2006).

[14] Y. Huang, J. Li, L. Wan, X. Meng, Y. Xie, Strengthening and toughening mechanisms of CNTs/Mg-6Zn composites via friction stir processing, Materials Science and Engineering A. **732**, 205-211 (2018). DOI: https://doi.org/10.1016/j.msea.2018.07.011

[15] A.M.K. Esawi, K. Morsi, A. Sayed, M. Taher, S. Lanka, Effect of carbon nanotube (CNT) content on the mechanical properties of CNT-reinforced aluminium composites, Composites Science and Technology **70** (16), 2237-2241 (2010).
DOI: https://doi.org/10.1016/j.compscitech.2010.05.004

[16] M. Chen, G. Fan, Z. Tan, C, Yuan, Q. Guo, D. Xiong, M. Chen, Q. Zheng, Z. Li, D. Zhang, Heat treatment behavior and strengthening mechanisms of CNT/6061Al composites fabricated by flake powder metallurgy, Materials Characterization **153**, 261-270 (2019). DOI: https://doi.org/10.1016/j.matchar.2019.05.017

[17] J.M. Jin, Discuss the catalytic mechanism of carbonate in solid carburizing agent again, Metal heat treatment (10), 37-41 (2000).
DOI: https://doi.org/10.13251/j.issn.0254-6051.2000.10.020

[18] X.X. Ye, B. Chen, J.H. Shen, J. Umed, K. Kondoh, Microstructure and strengthening mechanism of ultrastrong and ductile Ti-xSn alloy processed by powder metallurgy, Journal of Alloys and Compounds **709**, 381-393 (2017).
DOI: https://doi.org/10.1016/j.jallcom.2017.03.171

[19] Q. Ding, D. Zhang, Y. Pan, S. Hou, L. Zhuang, J. Zhang, Strengthening mechanism of age-hardenable Al–xMg–3Zn alloys, Materials Science and Technology **35** (9), 1071-1080 (2019).
DOI: https://doi.org/10.1080/02670836.2019.1612590

[20] R. Pérez-Bustamante, F. Pérez-Bustamante, M.C. Maldonado, R. Martínez-Sánchez, The effect of heat treatment on microstructure evolution in artificially aged carbon nanotube/Al2024 composites synthesized by mechanical alloying, Materials Characterization **126**, 28-34 (2017).
DOI: https://doi.org/10.1016/j.matchar.2017.01.006